# Myofibroblast Distribution in Dupuytren's Cords: Correlation With Digital Contracture

Liaquat Suleman Verjee, MBBS, Kim Midwood, PhD, Dominique Davidson, D. Phil., David Essex, MSc, Ann Sandison, MBBS, Jagdeep Nanchahal, PhD

**Purpose** Dupuytren's tissue has typically been described as being composed of myofibroblast-rich palmar nodules and relatively acellular tendon-like cords. We aimed to determine myofibroblast distribution (alpha-smooth muscle actin [α-SMA] positive cells) within Dupuytren's tissue and to correlate histologically defined α-SMA-positive nodules with digital contracture and recurrent disease.

**Methods** One hundred and three digital Dupuytren's cords (72 fasciectomy, 31 dermofasciectomy) were stained with anti–α-SMA antibody. The presence of α-SMA–positive nodules, their surface area, and α-SMA–positive cells were quantified throughout excised Dupuytren's tissue. Clinical data on diathesis, flexion deformity, and previous surgeries were collected.

**Results** Cords were nodular (66%) or non-nodular (34%). Nodular cords contained 1 (55%), 2 (33%), or 3 or more nodules (12%) composed of localized collections of cells. The mean total nodule surface area was 23 $mm^2$ (range, 1.3–105 $mm^2$). Nodules contained the highest number of α-SMA–positive cells (mean 97%, 2374 cells/$mm^2$) compared to peri-nodular areas (mean 32%, 763 cells/$mm^2$), and more distant cord (mean 8%, 495 cells/$mm^2$). Non-nodular cords contained 9% to 17% α-SMA–positive cells (mean 475–663 cells/$mm^2$), with higher numbers distally. There was greater digital contracture in patients with non-nodular cords. Thirty-six of 38 proximal interphalangeal (PIP) joint–marked samples had a nodule that co-localized with the PIP joint. Nodule size did not correlate with flexion deformity or with primary or recurrent disease.

**Conclusions** We found that two thirds of digital cords were nodular. Nodules were hypercellular, the majority being α-SMA–positive cells. Nodules varied in size and co-localized with the PIP joint. Cord was relatively cellular throughout; a proportion of these cells were α-SMA–positive and cells aligned with collagen fibers. Non-nodular cords correlated with significantly greater digital flexion contracture. We propose that cells in nodular cords contract and deposit extracellular matrix components. The matrix is then remodeled in shortened configuration, and as fixed flexion deformity develops, stress shielding eventually leads to myofibroblast apoptosis, and cord becomes less cellular. *(J Hand Surg 2009;34A:1785–1794. Copyright © 2009 by the American Society for Surgery of the Hand. All rights reserved.)*

**Key words** Alpha-smooth muscle actin (α-SMA), Dupuytren's contracture, Dupuytren's disease, myofibroblast, histopathology.

*From the Kennedy Institute of Rheumatology, Imperial College London, London, UK; St. John's Hospital, Livingston, Scotland; Imperial College School of Medicine, London, UK.*

Received for publication June 9, 2009; accepted in revised form August 13, 2009.

This work has been funded by grant awards from The Healing Foundation in association with the British Society for Surgery of the Hand, the Hammersmith Hospitals Trustees' Research Committee, and the Kennedy Institute of Rheumatology Trustees, Imperial College London. We are also grateful for support from the NIHR Biomedical Research Centre funding scheme.

No benefits in any form have been received or will be received related directly or indirectly to the subject of this article.

**Corresponding author:** Liaquat Suleman Verjee, MBBS, Kennedy Institute of Rheumatology, Imperial College London, 65 Aspenlea Road, London W6 8LH UK; e-mail: l.suleman-verjee@imperial.ac.uk.

0363-5023/09/34A10-0004$36.00/0
doi:10.1016/j.jhsa.2009.08.005

 

DUPUYTREN'S CONTRACTURE HAS classically been described as comprising hypercellular nodules, which often arise in the palm and mature as the disease progresses, to form acellular, tendon-like cord.[1] The cell that primarily contributes to digital contraction is the myofibroblast and, in Dupuytren's disease, it was first identified in nodules.[2] The most frequently used marker that characterizes myofibroblasts is alpha-smooth muscle actin ($\alpha$-SMA). The expression of $\alpha$-SMA in Dupuytren's nodules has been shown to correlate with the generation of contractile force.[3,4]

A nodule in the clinical sense manifests as a palpable subcutaneous mass and in the histological sense is defined as a dense collection of cells. Although nodules are often seen at the earliest stages of Dupuytren's disease, they do not necessarily correlate with histological nodules. Although some clinical nodules may well result from cell proliferation and extracellular matrix pushing upward on the skin to form a palpable nodule, others appear to arise from bunching up of the skin with contraction of the underlying fascia.[5]

Studies characterizing Dupuytren's disease have most often interpreted their findings within a histological framework defined by Luck as 3 distinct phases: proliferation, involution, and residual.[1] Dupuytren's tissue has been analyzed for the presence of myofibroblasts at different stages of the disease by both electron microscopy[2,6–8] and immunofluorescent staining.[6,9] The majority of these studies have demonstrated that the highly cellular nodule in the proliferation phase is composed almost entirely of myofibroblasts. Nodules remain highly cellular in the involution phase, in which the cells begin to align themselves along lines of stress within the tissue. Finally, in the residual phase, the nodules are described as almost acellular. Myofibroblasts are reported to disappear, leaving mature fibroblasts aligned with thick collagen bundles.

Dupuytren's tissue, however, might be more heterogenous than these histological phases imply. It has been reported that nodules vary substantially in size, exist as solitary or multiple nodules at various sites in the hand, and even in the absence of nodules, small groups of cells containing myofibroblasts are seen in advanced, tendon-like cords.[1,8] A more recent immunohistochemical study of 8 patient samples also showed that hypercellular zones within nodules have up to 40% $\alpha$-SMA–positive cells compared to 20% in less cellular regions of the same specimen.[10]

The clinical status of patients has been correlated with light and electron microscopic appearance of the excised Dupuytren's tissue.[8] Although a good correlation was suggested between morphological features and the duration of disease activity, objective clinical data and histological appearances have not been systematically quantified. It has also been suggested that highly cellular and proliferative Dupuytren's tissue seen histologically in primary disease correlates with disease recurrence when compared to less cellular fibrous tissue samples.[11]

The first aim of this study was to systematically characterize the distribution of $\alpha$-SMA–positive cells throughout excised Dupuytren's tissue. Our next objective was to determine whether there was a correlation between the presence of $\alpha$-SMA–rich nodules and the degree of preoperative flexion contracture, and finally, whether there was a relationship between the presence of these nodules and recurrent disease.

## METHODS

### Patient samples

In total, 103 digital cords were excised from 80 patients. The surgery was performed by 2 surgeons (J.N. and D.D.) between 2006 and 2008. Patients were recruited to the study after providing written consent. Specimens were collected from 2 sites: London and Edinburgh. The mean age in both groups was 64 years (range, 33–88 y) with an overall ratio of men to women of 3:1. Digital cords were mainly from ulna-sided disease (62, little finger; 30, ring finger; 7, middle finger; 2, index finger; and 2 from the thumb). Clinical data were recorded concurrently and are presented for each site to compare differences between the 2 groups in terms of diathesis,[12] previous surgery, and preoperative flexion contracture (Table 1). Overall, 53 patients were treated for both metacarpophalangeal (MCP) and proximal interphalangeal (PIP) joint contractures in the same digit, 11 patients were treated for isolated MCP joint contracture, and 29 were treated for isolated PIP joint contracture. Combined MCP, PIP, and distal interphalangeal (DIP) joint contractures in the same digit affected 5 patients, and both PIP joint and DIP joint contractures in the same digit were seen in 5 patients.

The indications for surgery included functional disability, PIP joint contracture greater than 30°, and progression of contracture. The same surgical selection criteria and surgical protocols were used by both surgeons. From 103 excised digital cords, the PIP joint was identified during surgery and marked in only the last 53 samples, and the MCP joint was identified and marked during surgery in only 2 cases.

### Immunohistochemistry

All tissue samples were fixed in formalin, longitudinally bisected, and embedded in paraffin wax, and 7-$\mu$m sections from the cut surface were processed for

**TABLE 1. Differences in Diathesis and Preoperative Contractures Compared in Samples From Edinburgh and London. Samples Were Grouped by Either Primary Disease or Recurrence (Following Previous Surgical Procedure As Indicated)**

| | Edinburgh | London | Combined |
|---|---|---|---|
| Diathesis (% incidence) | | | |
| Male | 70 | 90 | 76 |
| Family history (1st-degree relative) | 38 | 28 | 34 |
| Early onset <50 yrs | 46 | 41 | 44 |
| Bilateral disease | 75 | 83 | 78 |
| Garrod's pads | 38 | 44 | 40 |
| Preoperative flexion deformity (°) | | | |
| Mean MCP joint | 40 | 39 | 40 |
| Mean PIP joint | 65 | 55 | 62 |
| Mean DIP joint | 33 (n = 9) | 18 (n = 1) | 32 |
| Mean total flexion deformity | 93 | 63 | 83 |
| Fasciectomy (n) | 46 | 26 | 72 |
| Primary | 36 | 22 | 58 |
| Secondary, following previous: | 10 | 4 | 14 |
| Fasciotomy | 7 | 0 | 7 |
| Fasciectomy | 3 | 4 | 7 |
| Dermofasciectomy (n) | 28 | 3 | 31 |
| Primary | 13 | 0 | 13 |
| Secondary, following previous: | 15 | 3 | 18 |
| Fasciotomy | 6 | 0 | 6 |
| Fasciectomy | 6 | 2 | 8 |
| Dermofasciectomy—scar | 2 | 0 | 2 |
| Dermofasciectomy—firebreak | 1 | 1 | 2 |
| Total no. samples | 74 | 29 | 103 |

immunohistochemistry (Fig. 1). Sequential sections were stained with hematoxylin-eosin (H&E), mouse monoclonal anti–α-SMA antibody (Sigma, A2547), and mouse monoclonal anti-desmin (DAKO, M0760) antibody. Antibodies were detected using a 2-staged polymer system using enhancers (Sigma, HK519-YAK). Mouse serum at the same protein concentration as the monoclonal antibody solution was used as a negative control. Both α-SMA and desmin antibodies have been well characterized.[10,13,14]

### Analysis of distribution of α-SMA positive cells

Patient samples were grouped by the presence or absence of histological nodules. A nodule was defined as a distinct area of macroscopic α-SMA staining. Nodules were divided into 3 categories (1, 2, or ≥3 nodules). The total nodule surface area and total cord surface area were calculated, and cells were counted in each sample using an inverted microscope (Olympus, Tokyo, Japan) and OsteoMeasure*xp* v1.01 software, a Windows-based histomorphometry system (OsteoMetrics, Decatur, GA). In nodular cord, 3 areas were systematically analyzed for α-SMA–positive cell distribution: the nodules, peri-nodule (adjacent to the nodule), and the cord distal to the nodule (fibrous tissue furthest from any nodule). In non-nodular cord, 2 areas were analyzed: distal cord and proximal cord. Individual cells were counted in 6 fields of view within each defined region of interest at 20 times magnification. For each region of interest, the total number of cells, their distribution, and the percentage of the cells stained positive for α-SMA were also counted. In nodules with intense α-SMA staining, corresponding H&E sections were used to count the total number of cells. Vascu-

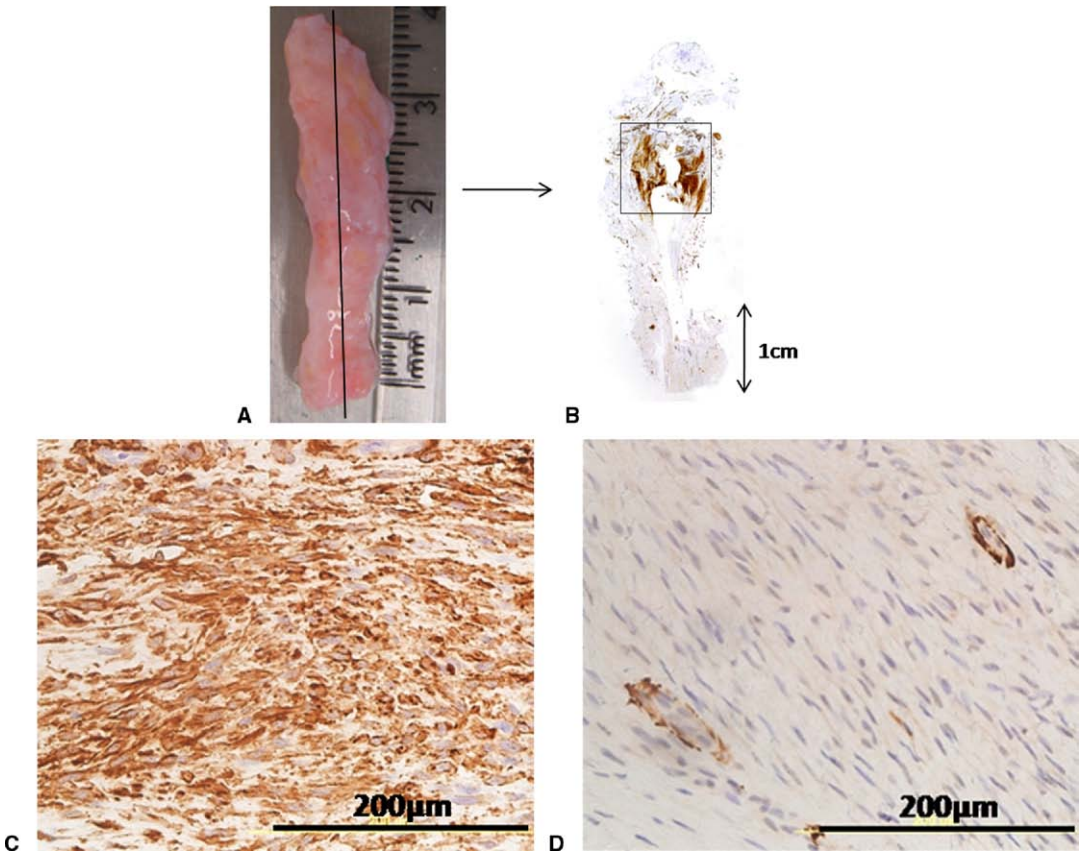


**FIGURE 1:** Cord samples were fixed in formalin and processed for immunohistochemistry. **A** Cords were longitudinally bisected (as shown by the line), and **B**, **C** histological sections were taken from the cut surface stained for α-SMA. **D** Serial sections were stained for desmin, which was used to distinguish between α-SMA positive cells in vessel walls and in stroma.

lar areas were excluded from the α-SMA–positive cell count because smooth muscle cells in vessel walls also stain positive for α-SMA. Desmin was used to delineate vascular areas seen on sequential sections stained with H&E and for α-SMA.[13]

### Statistical analysis

Statistical analysis was performed using software (Prism; GraphPad Software, San Diego, CA). Histological nodularity was compared with total flexion deformity in all samples, and within subgroups of primary and recurrent disease, geographical site, and gender. These analyses were done using either a Mann-Whitney nonparametric test, or an unpaired *t*-test, depending on the Gaussian distribution (determined by the Kolmogorov-Smirnov test). Analysis of single variance was performed when comparing nodule surface area with fasciectomy or dermofasciectomy, further divided by primary or recurrent disease. The association between total flexion deformity and total nodular or cord surface area was assessed using Spearman correlation. Significance was achieved if $p < .05$. All values are shown as the mean ± standard deviation.

## RESULTS

### Nodularity

Overall, two thirds of all samples were nodular. The size and number of nodules were extremely variable, with marked heterogeneity between samples (Fig. 2). Of the nodular samples, 55% had 1 nodule, 33% had 2 discrete nodules, and 12% had 3 or more nodules. Of the samples from London, 90% were nodular, compared to 55% from Edinburgh. The mean total nodular surface area was 23 $mm^2$ (range, 1.3–105 $mm^2$), and the mean total cord surface area was 143 $mm^2$ (range, 20–388 $mm^2$). Nodular cords were seen in 70% of men and 52% of women. There was no difference when comparing gender with total nodular ($p = .3$) or cord ($p = .4$) surface areas: men, mean nodule, 24 $mm^2$; mean cord, 147 $mm^2$; women, mean nodule, 19 $mm^2$; mean cord, 130 $mm^2$. Between geographical sites, there was also no significant difference in the total nodular surface area ($p = .9$) or total cord surface area ($p = .6$): Edinburgh (mean nodule, 25 $mm^2$; mean cord, 146 $mm^2$) and London (mean nodule, 20 $mm^2$; mean cord, 137 $mm^2$).

**FIGURE 2:** Longitudinal histological sections through digital cords, staining for α-SMA. Of a total of 103 cord samples, 66% were nodular and 34% were non-nodular. There was considerable variation in both number of nodules and nodule size (surface area range, 1.3–105 $mm^2$).

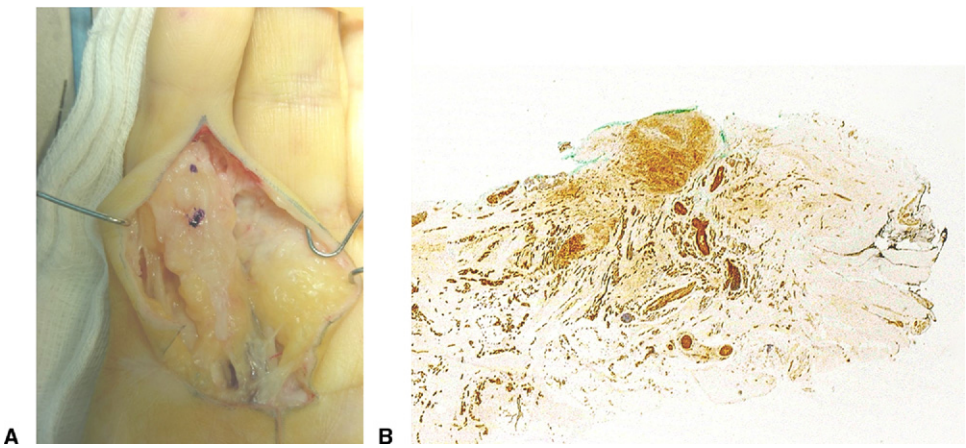


**FIGURE 3: A** Dupuytren's fasciectomy with PIP joint and distal end marked with ink during surgery. **B** Co-localization of PIP joint (green ink marking) and α-SMA nodule is seen on histological section. Of the 38 cords, 36 (95%) were nodular cords in which nodules co-localized with the PIP joint.

There was no significant difference ($p = .3$) in mean cord surface area between nodular samples (149 $mm^2$) and non-nodular samples (129 $mm^2$).

### Proximal interphalangeal joint co-localization

Of the 103 excised digital cords, only in the last 53 samples was the PIP joint identified during surgery and its position marked relative to cord (Fig. 3). Thirty-eight were nodular samples, and in 36 of these, the PIP joint co-localized with a nodule. Two samples were also marked for the MCP joint, and both showed co-localization with a nodule (not shown). Although no cord samples were marked during surgery for the DIP joint, nodular cords were seen in 6 of 10 patients with DIP joint contractures (3 had multiple nodules).

### α-SMA distribution throughout Dupuytren's tissue

At a cellular level, Dupuytren's tissue is also quite heterogenous (Fig. 4). In nodular cords, the nodules (Fig. 4A) were consistently hypercellular (mean,

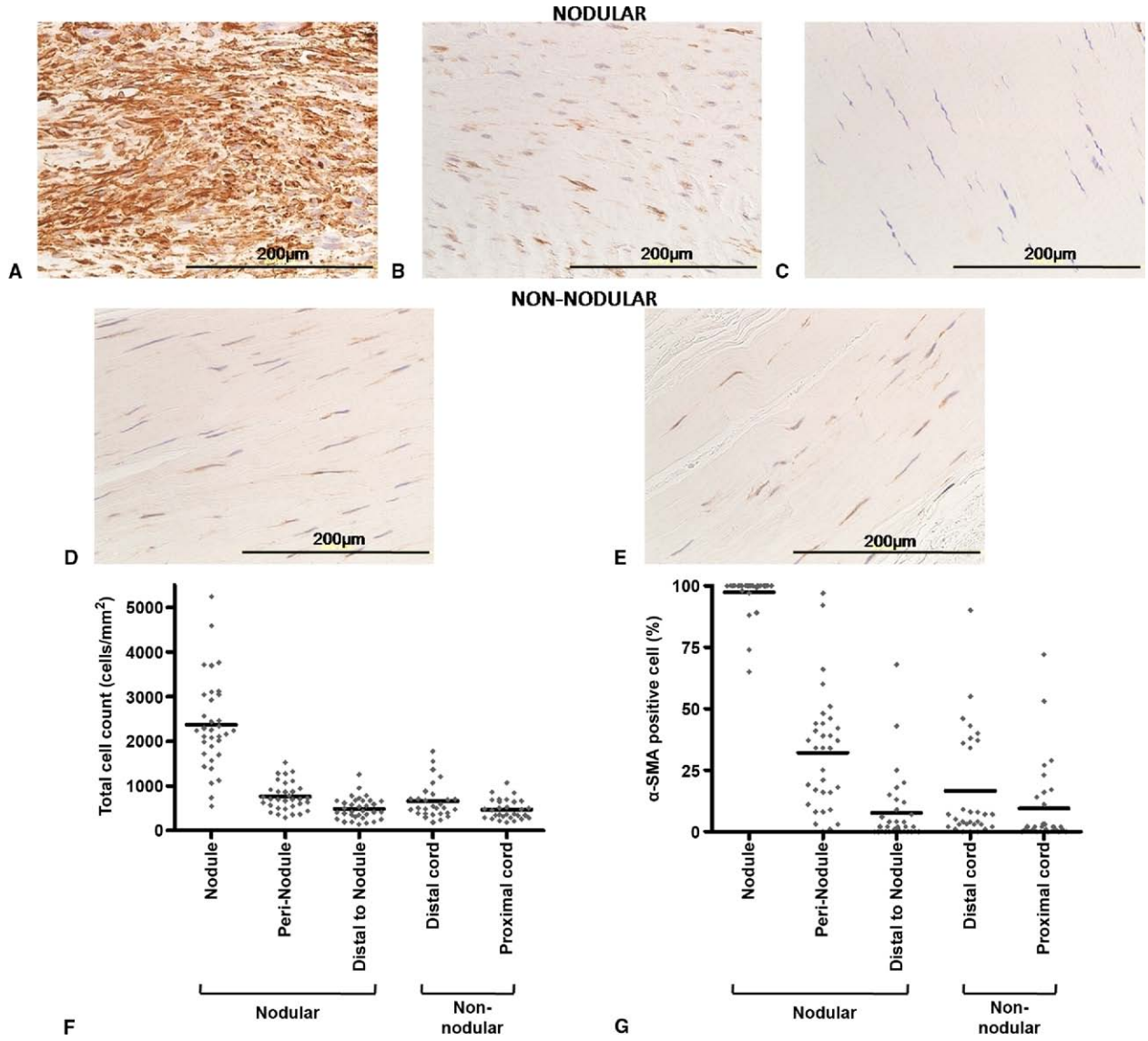


**FIGURE 4:** Representative panels of systematically analyzed regions in **A**–**C** nodular and **D**, **E** non-nodular cord. Corresponding **F** total cell counts and **G** percentage of α-SMA–positive cells. In nodular cords, **A** the nodules were consistently cellular (2,374 ± 1,021 cells/mm$^2$), and on average, 97% of cells stained positive for α-SMA. There was marked heterogeneity **B** outside the nodules, with 32% α-SMA–positive cells peri-nodule (mean total cells, 763 ± 313 cells/mm$^2$). **C** Cord distant from any nodule had 8% α-SMA–positive cells (mean total cells, 495 ± 246 mm$^2$). In non-nodular cord, a higher number of cells was seen at **D** the distal end (663 ± 392 cells/mm$^2$) than **E** proximally (475 ± 221 cells/mm$^2$). Significantly more α-SMA–positive cells were seen at the distal end (17%) compared to the proximal end (9%). This correlated with the PIP joint in some (33%), but not all, samples. **F**, **G** Bars represent mean counts and percentages.

2374 ± 1021 cells/mm$^2$), with cells densely packed together in whorls and a mean of 97% cells staining positive for α-SMA. In the peri-nodular area (Fig. 4B), there were relatively fewer cells (mean, 763 ± 313 cells/mm$^2$) and, on average, 32% of these were positive for α-SMA. Cord distal from any nodule (Fig. 4C) was the least cellular (mean, 495 ± 246 mm$^2$), with a mean of 8% α-SMA–positive cells. Cells in cord, distal from a nodule, were aligned with the collagen fibers. Non-nodular cord was relatively cellular throughout (mean distal cord, 663 ± 392 cells/mm$^2$; mean proximal cord, 475 ± 221 cells/mm$^2$), and more α-SMA–positive cells (17%) were seen at the distal end (Fig. 4D) compared to 9% in proximal cord (Fig. 4E). This pattern of more α-SMA–positive cells at the distal end correlated in some (33%), but not all cases, with the PIP joint. The difference in cell distribution or percent α-SMA–positive cell number remained unchanged when comparisons were made between sites and with gender (not shown).

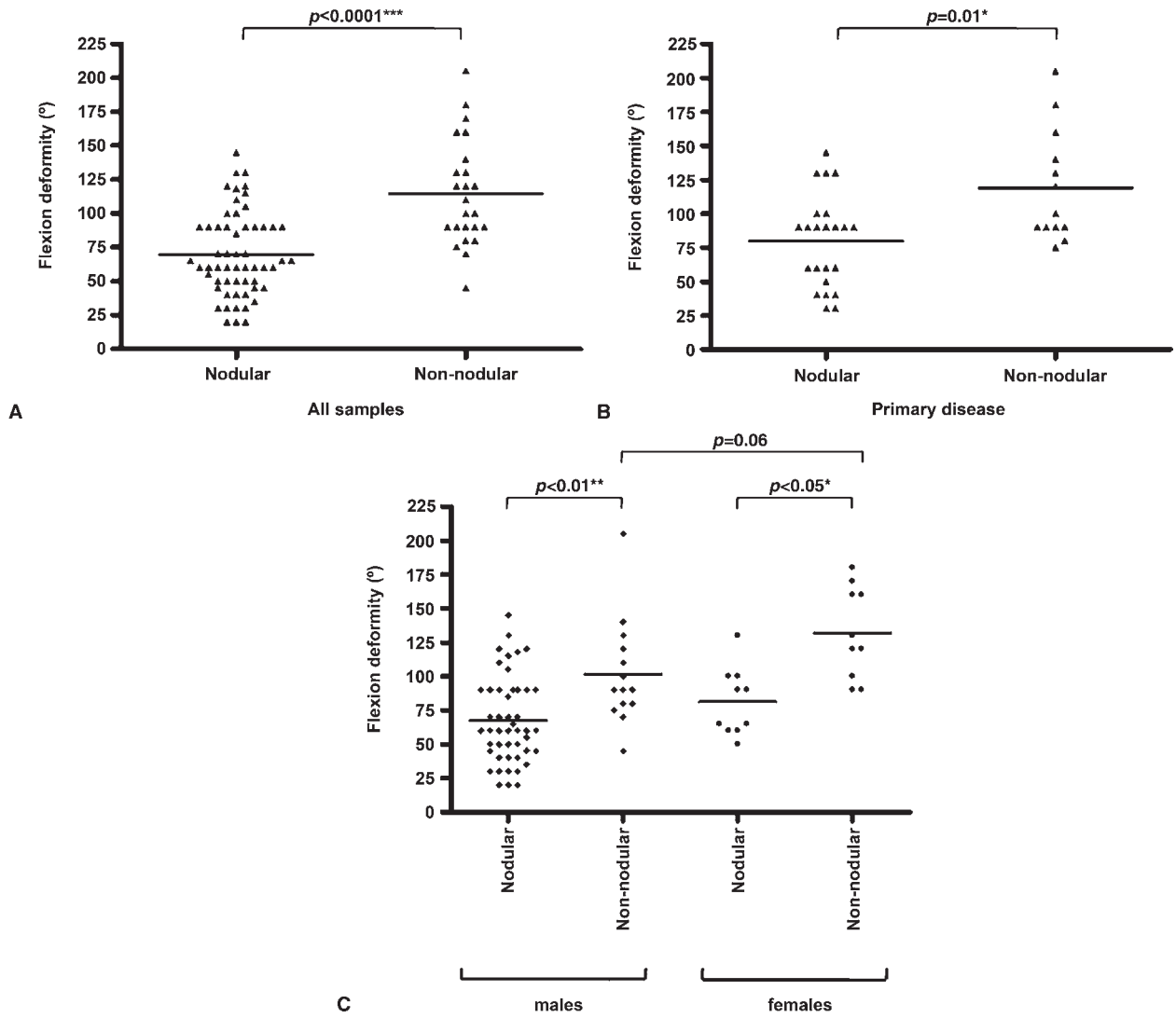


**FIGURE 5:** There was a significant difference in the flexion contracture and cord nodularity in **A** all samples and **B** primary disease. **C** In both males and females, there was a significant difference between non-nodular and nodular cords. However, there was no significant difference in only non-nodular cords between men and women. Bars represent mean values.

### Nodularity correlated with digital contraction

There was a significant correlation ($p < .0001$) between non-nodular cords and digital contracture (mean flexion deformity, 114° ± 39°) compared to nodular cords (mean flexion deformity, 70° ± 31°) (Fig. 5). This significant difference was maintained with samples from primary disease ($p = .01$). Nodular cords showed no difference ($p = .11$) in degree of contracture between geographical sites (Edinburgh, 76° ± 33; London: 62° ± 26°), whereas non-nodular cords were almost exclusively from Edinburgh (not shown). There was no correlation between digital contracture and either total nodule surface area ($p = .2$) or total cord surface area ($p = .3$).

Pre-operatively, women had a significantly greater ($p = .002$) mean total flexion contracture than men (women, 107° ± 39°; men, 75° ± 36°). A greater flexion contracture was seen in the non-nodular cords of both men ($p < .01$) and women ($p < .05$) when compared to nodular cords. In men, the mean flexion contracture was 102° ± 39° in non-nodular samples and 67° ± 32° in nodular samples. In women, the mean non-nodular flexion contracture was 132° ± 34° in non-nodular samples and 81° ± 25° in nodular samples.

### Nodularity correlated with primary or recurrent disease

Nodules were seen as frequently in fasciectomy samples (67%) as they were in dermofasciectomy samples (66%). When further subdivided into primary or recurrent disease, approximately two thirds in both groups

**TABLE 2. Nodular and Non-Nodular Cords Grouped by Primary Procedure or Secondary Procedure (for Recurrent Disease). Mean Nodule Surface Areas for Primary and Recurrent Disease Also Included**

| | Total (n) | Non-Nodular | Nodular | Nodular Surface Area ($mm^2$) |
|---|---|---|---|---|
| Fasciectomy | 72 | 33% | 67% | |
| Primary | 58 | 19 (33%) | 39 (67%) | 23 ± 21 |
| Secondary, following previous: | 14 | 5 (36%) | 9 (64%) | 17 ± 16 |
| Fasciotomy | 7 | 2 | 5 | |
| Fasciectomy | 7 | 3 | 4 | |
| Dermofasciectomy | 31 | 34% | 66% | |
| Primary | 13 | 5 (38%) | 8 (62%) | 33 ± 29 |
| Secondary, following previous: | 18 | 5 (31%) | 11 (69%) | 22 ± 30 |
| Fasciotomy | 6 | 3 | 3 | |
| Fasciectomy | 8 | 2 | 6 | |
| Dermofasciectomy—scar tissue* | 2 | 2 | | |
| Dermofasciectomy—firebreak | 2 | | 2 | |
| Total no. samples | 103 | 34% | 66% | 24 ± 23 |

*Excluded from non-nodular count.

were still classified as nodular (Table 2). Two dermofasciectomy samples were excluded because the surgery was performed for cutaneous scar contracture and not true recurrence. The overall mean total nodular surface area was not significantly different ($p = .5$) between primary (mean, 24 ± 23 $mm^2$) and recurrent disease (mean, 20 ± 24 $mm^2$). Total cord surface area was also not significantly different ($p = .5$) between primary (mean, 144 ± 71 $mm^2$) and recurrent disease (mean, 140 ± 98 $mm^2$). The nodular surface area was not significantly different ($p = .54$) in primary dermofasciectomy samples (mean, 33 ± 29 $mm^2$) as compared to either primary fasciectomy (mean, 23 ± 21 $mm^2$), secondary fasciectomy (mean, 17 ± 16 $mm^2$) or dermofasciectomy following recurrent disease (mean, 22 ± 30 $mm^2$). There was no significant difference ($p = .09$) in flexion deformity between samples from primary (mean, 76° ± 41°) and recurrent disease (mean, 88° ± 37°).

## DISCUSSION

The comparison of Dupuytren's samples from Edinburgh and London highlighted differences between patients from the 2 sites. Of the 103 digital cords analyzed, the majority were from Edinburgh (n = 74), and the remainder from London (n = 29). In London, 90% of patients were men, the digits tended to be less flexed (mean flexion deformity, 63° ± 26°), and 3 out of every 4 patients presented with primary disease. Most of the patients (26/29) were treated by fasciectomy, and the remaining 3 by dermofasciectomy. In comparison, 70% of patients in Edinburgh were men, and the overall flexion deformity was significantly greater (93° ± 40°). There were more women in the Edinburgh cohort, and they presented with a significantly greater mean flexion deformity than men ($p = .002$). This might reflect delayed presentation in women, rather than selection bias. Approximately one third of samples from Edinburgh were obtained from patients with recurrence following previous surgery, and half of these were following previous fasciotomy. Although previous fasciectomy accounted for most of the remaining recurrences, both sites had 1 recurrence following a firebreak dermofasciectomy. There was no difference in digital distribution between Edinburgh and London, and the diathesis was similar (Table 1).

The immunohistochemical analysis of myofibroblast distribution in Dupuytren's tissue using α-SMA to identify myofibroblasts has previously been carried out in a small study of 8 patient samples.[10] Although α-SMA is the most frequently used marker for myofibroblasts, bundles of contractile actin microfilaments alone cannot reliably distinguish between myofibroblasts and vascular smooth muscle cells, especially in the nodule where mixed populations exist. The 2 cell populations can be distinguished at an ultrastructural level by the presence of fibronexi,[15] specialized areas on the surface of myofibroblasts. However, because our objective was to assess myofibroblast distribution throughout cord tissue, ultrastructural imaging would

have limited analysis to small areas of tissue. Desmin is an established marker for smooth muscle cells in blood vessel walls,[13] although a proportion of desmin-positive myofibroblasts have also been shown to be present around capillaries and blood vessels in proliferating Dupuytren's nodules.[6,16] We used desmin staining to delineate vascular areas seen on sequential sections stained with H&E and for $\alpha$-SMA; therefore, stromal $\alpha$-SMA–positive myofibroblasts were more reliably identified and counted.

We found that two thirds of all cords were nodular, and nodules existed as tiny foci of cells or as larger single or even multiple nodules. The total nodular surface area range varied from 1.3 to 105.0 mm.[2] Nodules were not significantly different in size when comparing between Edinburgh and London or between men and women. Nodular cords were also not significantly different in size compared to non-nodular cords. At a cellular level, nodules were hypercellular (2374 cells/mm$^2$), with a mean of 97% $\alpha$-SMA–positive cells. It has previously been reported that myofibroblasts made up the majority of cells in nodules,[1,2,6,7,17] and that cord tissue is almost acellular and tendon-like.[1] However, there was considerable heterogeneity, as evidenced by the wide range of cellularity. We found that non-nodular cord was cellular throughout, with on average 9% (proximal) and 17% (distal) of cells positive for $\alpha$-SMA. The $\alpha$-SMA–positive cells were distributed among collagen fibers, aligned along a longitudinal axis. This heterogeneity is of some importance because frequent comparisons are made between nodule and cord on the basis of gross morphology.

Although nodules have been previously reported in digits,[1,8] typically Dupuytren's disease has been described as comprising nodules that arise in the palm and mature into relatively acellular cords.[1] However, we found a single nodule (55%), 2 nodules (33%), and often 3 or more nodules (12%) within mature cords. Therefore, it is unlikely that palmar nodules alone can account for the pathogenesis of Dupuytren's contracture. It seems more plausible that Dupuytren's tissue is heterogenous, and multiple nodules located in different regions of digital cord tissue cumulatively contribute to digital contraction.

When comparing histological findings and the patients' clinical status, we found that non-nodular cords were associated with greater digital contractures compared to nodular cords ($p < .0001$). This significantly greater digital contracture in non-nodular cords was also evident when considering only primary disease samples and in both men and women. This implies that non-nodular cords might reflect the end-stage process following extracellular matrix remodeling, whereas the presence of myofibroblast-rich nodules might represent more active and less contracted digital cords. However, in nodular samples, no further correlation was found between nodule size and digital contracture, and this might represent different stages of disease in patients at time of surgery. Unfortunately, it is not possible to verify the progression of myofibroblast numbers and distribution in a given patient over time.

We also found that 95% (36/38) of nodules co-localized with the PIP joint, and nodules also co-localized with the MCP joint in the only 2 cases marked during surgery for the MCP joint. The presence of nodules in line with digital rays and in close proximity to the PIP joint and MCP joint has been previously described.[1,8] One explanation for PIP joint and nodule co-localization is based on the understanding that myofibroblasts perceive and thrive on tension.[18–22] In early or active disease, tension might act intermittently on Dupuytren's tissue as active extension of the PIP joint offers resistance against the thickened, contracted palmar fascia. The increased tension sensed by cells might promote myofibroblast differentiation through recruitment of $\alpha$-SMA to stress fibers and specialized attachment site formation under strict control of TGF$\beta$-1 and fibronectin-EDA. This in turn leads to greater force generation. A densely packed cellular nodule could then theoretically exert sufficient force to promote or sustain digital contracture. The cells then remodel the surrounding matrix to a more shortened configuration. This would be supported by the increased expression of matrix metalloproteinases in Dupuytren's nodules and cord.[23–26] The resulting increased flexion deformity would impair function and the reduced movement at the joint would in turn lead to a reduction in tension sensed by nodular myofibroblasts. This can be considered as a form of stress shielding, which in wound healing has been shown to result in myofibroblast apoptosis after re-epithelialization.[27] Furthermore, in a rat model in which the wound was splinted with a sutured metal template, thereby preventing tension release, myofibroblast apoptosis was inhibited, and subsequent splint removal was followed by a reduction in myofibroblast numbers.[28] It is, therefore, conceivable that with advanced digital contractures, reduced tension through limited active joint extension might similarly lead to myofibroblast apoptosis, whereby myofibroblast-rich nodules fail to persist. This might explain the progression from nodular to non-nodular cords and it could also explain why patients with non-nodular cords tended to have more severe flexion deformities.

Nodules were seen in two thirds of cords in both primary and recurrent disease, and there was also no significant difference in digital contracture between primary and recurrent disease. Recurrence was seen following previous fasciectomy (n = 15), fasciotomy (n = 13), and in 2 cases, firebreak dermofasciectomy for previous recurrence, both cords being nodular. There was also no difference in nodular surface area between primary dermofasciectomy samples, primary fasciectomy, secondary fasciectomy, or dermofasciectomy following recurrent disease (p = .5). These histological findings suggest similar pathogenesis in both primary and recurrent disease and that nodularity is not downregulated following previous surgery. Indeed, the increased motion after the initial surgery might facilitate myofibroblast differentiation and persistence. It is possible that residual, unexcised Dupuytren's tissue following fasciotomy, fasciectomy, and firebreak dermofasciectomy might serve as a trigger for recurrence. This might also explain why radical dermofasciectomy has a lower rate of recurrence (1–5%)[29–31] than firebreak dermofasciectomy (12%)[32] or fasciectomy (40–50%).[29,33,34] It would be interesting to compare the myofibroblast distribution in the cords of any of our fasciectomy patients who develop recurrence in the future with the primary excision specimens.

## REFERENCES


1. Luck JV. Dupuytren's contracture; a new concept of the pathogenesis correlated with surgical management. J Bone Joint Surg 1959; 41A:635–664.
2. Gabbiani G, Majno G. Dupuytren's contracture: fibroblast contraction? An ultrastructural study. Am J Pathol 1972;66:131–146.
3. Tomasek J, Rayan GM. Correlation of alpha-smooth muscle actin expression and contraction in Dupuytren's disease fibroblasts. J Hand Surg 1995;20A:450–455.
4. Rayan GM, Tomasek JJ. Generation of contractile force by cultured Dupuytren's disease and normal palmar fibroblasts. Tissue Cell 1994;26:747–756.
5. McGrouther DA. The microanatomy of Dupuytren's contracture. Hand 1982;14:215–236.
6. Schurch W, Skalli O, Gabbiani G. Cellular biology. In: McFaralane RM, McGrouther DA, Flint MH, eds. Dupuytren's disease: biology and treatment. London: Churchill Livingstone, 1990:31–47.
7. Iwasaki H, Muller H, Stutte HJ, Brennscheidt U. Palmar fibromatosis (Dupuytren's contracture). Ultrastructural and enzyme histochemical studies of 43 cases. Virchows Arch A Pathol Anat Histopathol 1984;405:41–53.
8. Chiu HF, McFarlane RM. Pathogenesis of Dupuytren's contracture: a correlative clinical-pathological study. J Hand Surg 1978;3:1–10.
9. Tomasek JJ, Schultz RJ, Episalla CW, Newman SA. The cytoskeleton and extracellular matrix of the Dupuytren's disease "myofibroblast": an immunofluorescence study of a nonmuscle cell type. J Hand Surg 1986;11A:365–371.
10. Hindman HB, Marty-Roix R, Tang JB, Jupiter JB, Simmons BP, Spector M. Regulation of expression of alpha-smooth muscle actin in cells of Dupuytren's contracture. J Bone Joint Surg 2003;85B:448–455.
11. Rombouts JJ, Noel H, Legrain Y, Munting E. Prediction of recurrence in the treatment of Dupuytren's disease: evaluation of a histologic classification. J Hand Surg 1989;14A:644–652.
12. Hindocha S, Stanley JK, Watson S, Bayat A. Dupuytren's diathesis revisited: evaluation of prognostic indicators for risk of disease recurrence. J Hand Surg 2006;31A:1626–1634.
13. Christen T, Verin V, Bochaton-Piallat M, Popowski Y, Ramaekers F, Debruyne P, et al. Mechanisms of neointima formation and remodeling in the porcine coronary artery. Circulation 2001;103:882–888.
14. Skalli O, Ropraz P, Trzeciak A, Benzonana G, Gillessen D, Gabbiani G. A monoclonal antibody against alpha-smooth muscle actin: a new probe for smooth muscle differentiation. J Cell Biol 1986;103: 2787–2796.
15. Tomasek JJ, Haaksma CJ. Fibronectin filaments and actin microfilaments are organized into a fibronexus in Dupuytren's diseased tissue. Anat Rec 1991;230:175–182.
16. Shum DT, McFarlane RM. Histogenesis of Dupuytren's disease: an immunohistochemical study of 30 cases. J Hand Surg 1988; 13A:61–67.
17. Tomasek JJ, Vaughan MB, Haaksma CJ. Cellular structure and biology of Dupuytren's disease. Hand Clin 1999;15:21–34.
18. Goffin JM, Pittet P, Csucs G, Lussi JW, Meister JJ, Hinz B. Focal adhesion size controls tension-dependent recruitment of alpha-smooth muscle actin to stress fibers. J Cell Biol 2006;172:259–268.
19. Hinz B. Formation and function of the myofibroblast during tissue repair. J Invest Dermatol 2007;127:526–537.
20. Hinz B. Masters and servants of the force: the role of matrix adhesions in myofibroblast force perception and transmission. Eur J Cell Biol 2006;85:175–181.
21. Gabbiani G. The myofibroblast in wound healing and fibrocontractive diseases. J Pathol 2003;200:500–503.
22. Tomasek JJ, Gabbiani G, Hinz B, Chaponnier C, Brown RA. Myofibroblasts and mechano-regulation of connective tissue remodelling. Nat Rev Mol Cell Biol 2002;3:349–363.
23. Johnston P, Chojnowski AJ, Davidson RK, Riley GP, Donell ST, Clark IM. A complete expression profile of matrix-degrading metalloproteinases in Dupuytren's disease. J Hand Surg 2007;32A:343–351.
24. Ulrich D, Hrynyschyn K, Pallua N. Matrix metalloproteinases and tissue inhibitors of metalloproteinases in sera and tissue of patients with Dupuytren's disease. Plast Reconstr Surg 2003;112:1279–1286.
25. Tarlton JF, Meagher P, Brown RA, McGrouther DA, Bailey AJ, Afoke A. Mechanical stress in vitro induces increased expression of MMPs 2 and 9 in excised Dupuytren's disease tissue. J Hand Surg 1998;23B:297–302.
26. Johnston P, Larson D, Clark IM, Chojnowski AJ. Metalloproteinase gene expression correlates with clinical outcome in Dupuytren's disease. J Hand Surg 2008;33A:1160–1167.
27. Desmouliere A, Redard M, Darby I, Gabbiani G. Apoptosis mediates the decrease in cellularity during the transition between granulation tissue and scar. Am J Pathol 1995;146:56–66.
28. Carlson MA, Longaker MT, Thompson JS. Wound splinting regulates granulation tissue survival. J Surg Res 2003;110:304–309.
29. Tonkin MA, Burke FD, Varian JP. Dupuytren's contracture: a comparative study of fasciectomy and dermofasciectomy in one hundred patients. J Hand Surg 1984;9B:156–162.
30. Brotherston TM, Balakrishnan C, Milner RH, Brown HG. Long term follow-up of dermofasciectomy for Dupuytren's contracture. Br J Plast Surg 1994;47:440–443.
31. Hall PN, Fitzgerald A, Sterne GD, Logan AM. Skin replacement in Dupuytren's disease. J Hand Surg 1997;22B:193–197.
32. Ullah AS, Dias JJ, Bhowal B. Does a 'firebreak' full-thickness skin graft prevent recurrence after surgery for Dupuytren's contracture? A prospective, randomised trial. J Bone Joint Surg 2009;91B: 374–378.
33. Hueston JT. Limited fasciectomy for Dupuytren's contracture. Plast Reconstr Surg Transplant Bull 1961;27:569–585.
34. Foucher G, Cornil C, Lenoble E. Open palm technique for Dupuytren's disease. A five-year follow-up. Ann Chir Main Memb Super 1992;11:362–366.